Multi-model probability assessments in the Long-Valley volcanic region (CA)

Andrea Bevilacqua[1], Marcus Bursik[1], Abani K. Patra[2], E. Bruce Pitman[3], Qingyuan Yang[1]

(1) University at Buffalo, Department of Geology
(2) University at Buffalo, Department of Mechanical and Aerospace Engineering
(3) University at Buffalo, Department of Materials Design and Innovation

Project Hazard SEES: Persistent volcanic crises resilience in the face of prolonged and uncertain risk,
National Science Foundation, 2015 - 2018.

ID 634, PE51A-8, III.1 Forecasting volcanic eruptions
18 August 2017, Portland (OR)

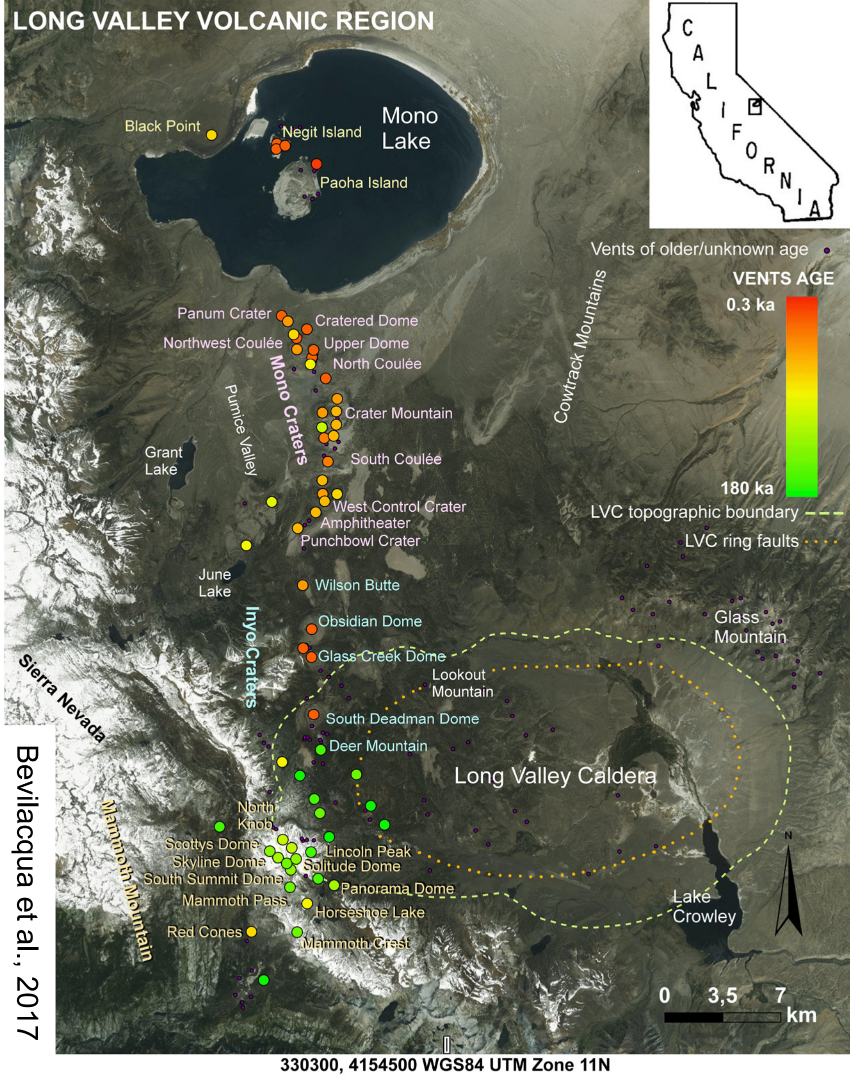

Bevilacqua et al., 2017

- The Long Valley volcanic region -

Long Valley caldera (LVC), was created by the eruption of >650km^3 tephra ~ 760ka (Bishop tuff).

After 180ka, the eruptions have been mostly localized at Mammoth Mountain, and its periphery and along the Mono-Inyo Craters volcanic chain, stretching ~45km North outside the caldera, towards Mono Lake.

The most recent period of unrest started in 1978 - several seismic swarms in LVC and below Mammoth Mountain, and diffuse volcanic CO_2 emissions.

We produce long-term forecasting models for the timing and location of future eruptions, with uncertainty.

The models are doubly stochastic,
i.e. each sample is made in two steps:
A) the random choice of the epistemic uncertainty,
B) the random determination of the forecasts, conditional on A).

All probability values will have
confidence intervals due to the uncertainties.

- Eruptive record uncertainty model -

The radio-isotopic age of past eruptions is affected by uncertainty, but constrained by the stratigraphic sequence.

A Monte Carlo simulation samples the ages and resamples those which contradict stratigraphic constrains.
This enables the reconstruction of a stochastic record of 134 events after 180 ka including inter-event dependence.

Our definition of event is an eruptive activity which is interrupted by evidence of quiescence of yearly scale.
Sometimes multiple units can correspond to a single event, or single units can correspond to multiple events.

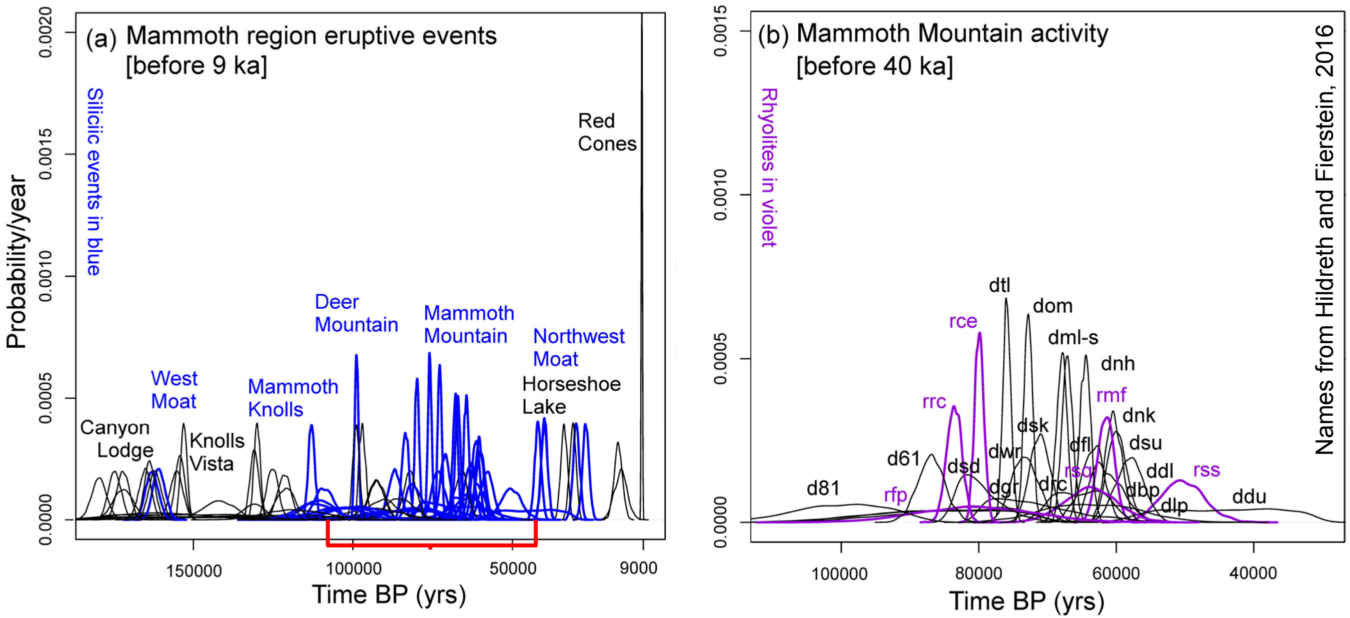

The first and older part of eruptive record is related to:
Mammoth region (81 events)

Mammoth Mountain
26^{+3} events [110 - 40] ka

Mammoth periphery
52 events [180 - 9] ka

The figure is based on 10^4 samples.

- Eruptive record uncertainty model -

The second part of eruptive record is related to
Mono region (53 events)

Mono Lake	*8 events*	[14 - 0.2] ka
Inyo craters	*3 events*	[5.5 - 0.6] ka
Mono domes	*23^{+2} events*	[65 - 0.6] ka
Wilson Creek Formation	*21^{-4} events*	[65 - 13] ka

The Wilson Creek Formation preserves 5 sequences of ash beds, most of them tracing back to Mono-Inyo craters.

This enabled us to include older eruptions whose vents can be buried.

The figure is based on 10^4 samples.

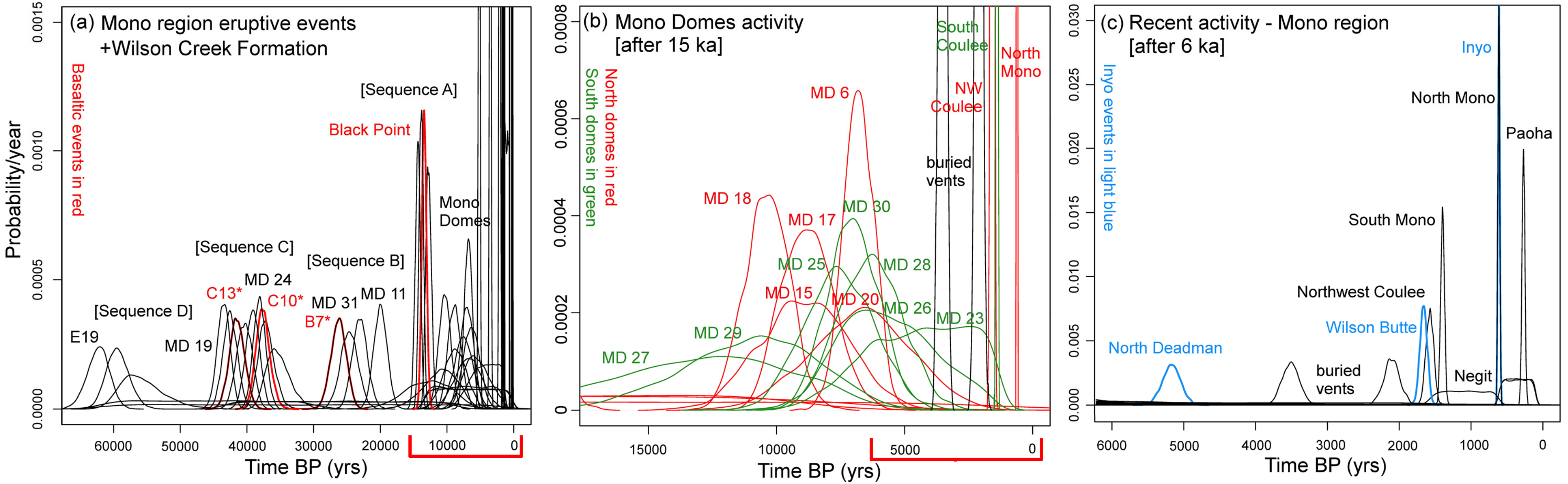

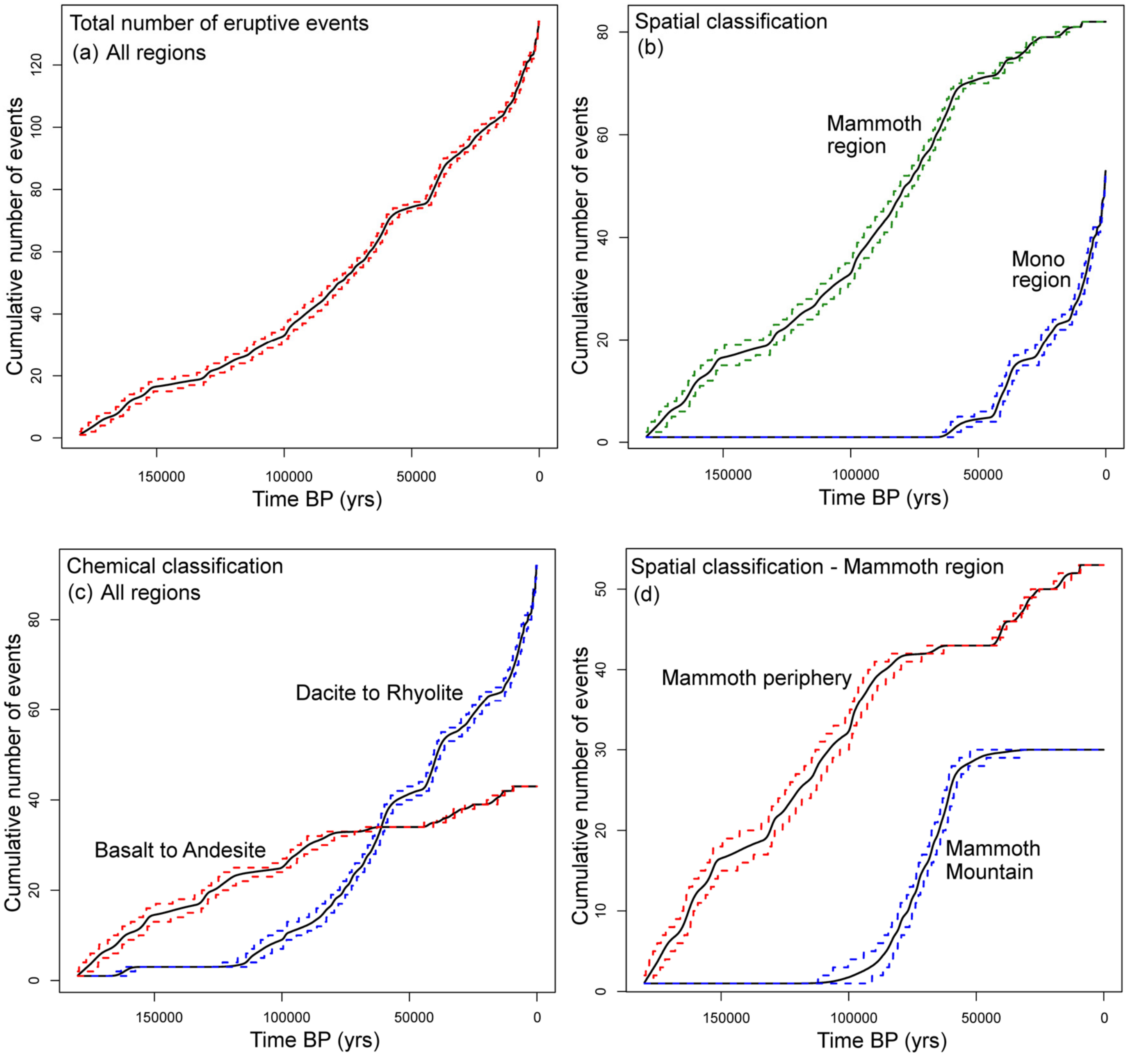

- Cumulative event number -

Mean curves, with 5%ile and 95%ile values, as a function of time. Based on 2500 samples.

The slope of the plot (a) is significantly regular, except for a weak apparent acceleration of the activity.

Plot (b) shows the increase of activity in Mono region after 60 ka, complementary to an apparent decrease in Mammoth region.

In plot (c) the rate for the silicic events is approximately twice the rate of basaltic events.

In plot (d) Mammoth Mountain activity is mostly constrained between 100 ka and 50 ka.

At [65 - 40] ka can be seen a stop in the activity of the Mammoth periphery.

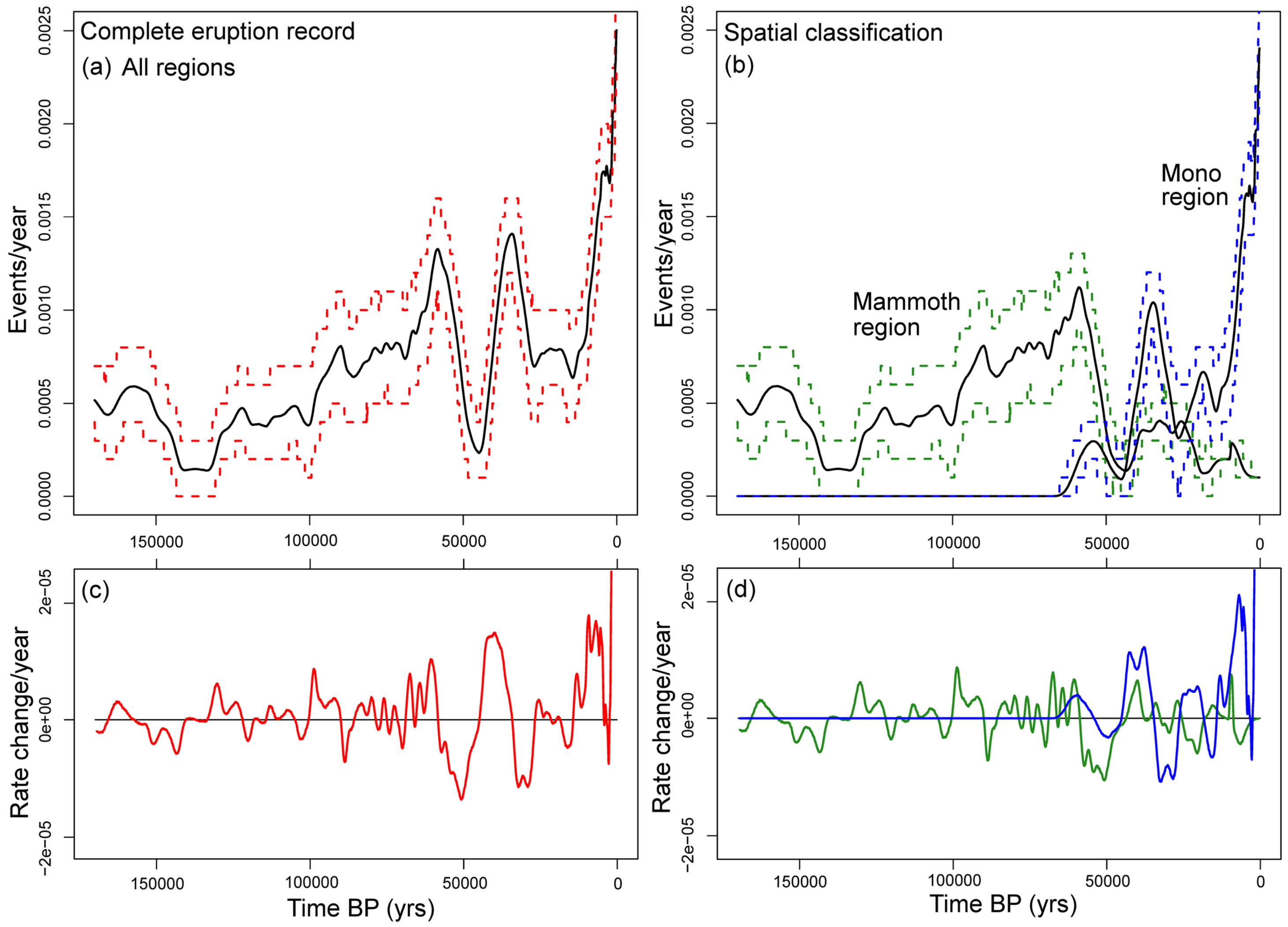

- Event rate -

Including uncertainty.

In plot (a) after a rate reduction at 140-130 ka, there was regular rise until 60 ka, then a drop down and a new burst at 40-30 ka, reaching 1/750 yr^{-1} rate.

After 15 ka, there was a burst twice the previous, to 1/400 yr^{-1}.

Plot (b) shows that the rise of new activity after 50 ka is mostly related to Mono region, in four clusters.

Rate change plots (c and d) show an alternation of negatively and positively valued intervals, pulsing with a ~15-20 kyr period .

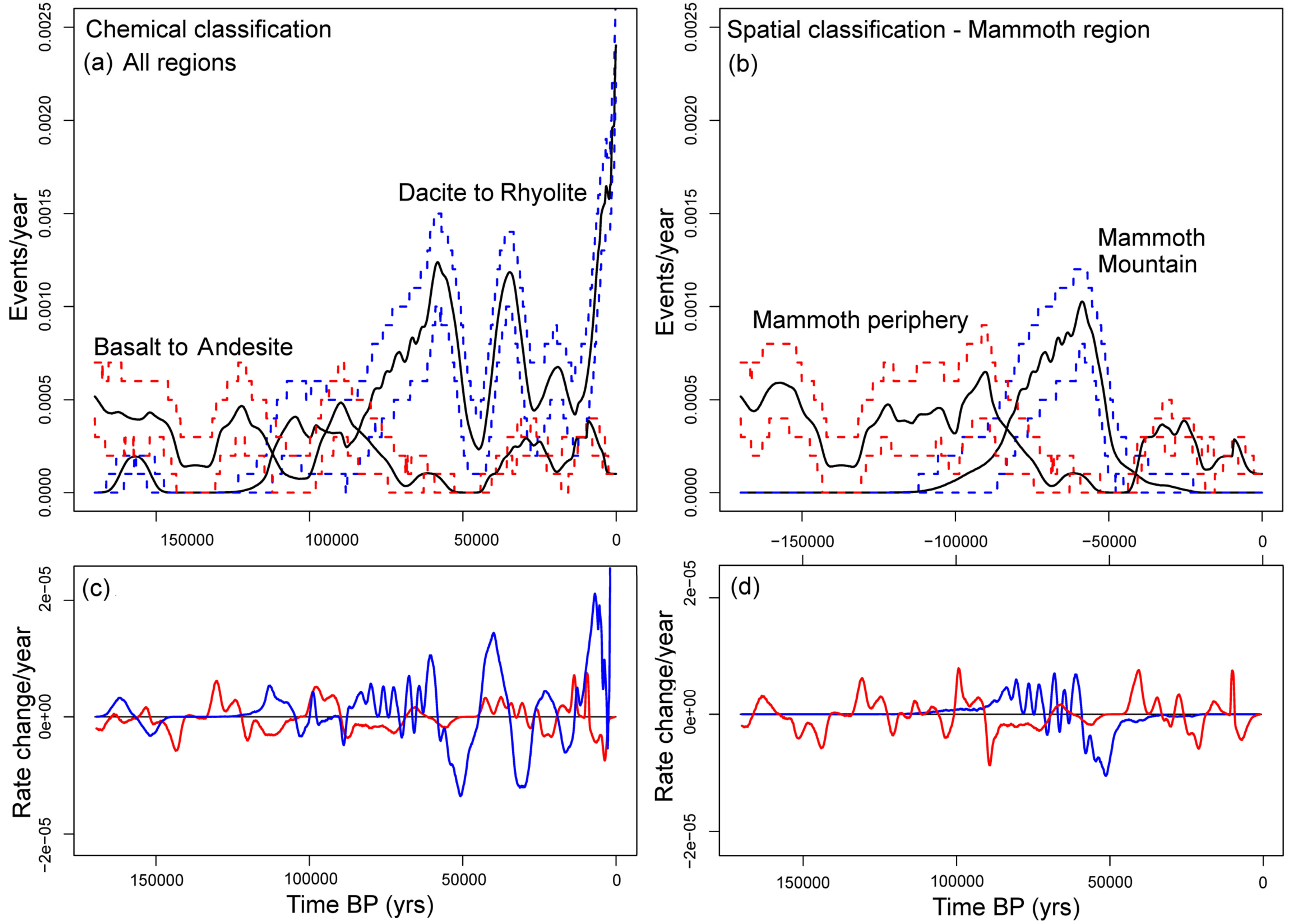

- Event rate -

Including uncertainty.

In plot (a) basaltic activity has 4-5 clusters, with a gap when the silicic activity rises to a maximum at 60 ka.

Three bursts in the more recent times are evident.

In plot (b) decrease of peripheral activity is clear at 80-40 ka.

In plot (c) an alternation of basaltic and silicic activity has peaks of in silicic activity corresponding to valleys in basaltic activity and vice versa.

Exceptions are before 130 ka and at 60-40 ka, with a more coupled behavior.

- Cox processes based on moving averages -

MODEL 1

The intensity function λ(t), which is the average rate of our forecasting model at time t, is defined by the ratio *#events* / T on a left window [t-T, t]. T is the only parameter.

MODEL 1B - (adaptive time-window correction)

The intensity function λ(t) is the ratio $k / (t - t_{n-k})$, where *k* is a parameter, and t_n is the time of the last event occurred before time t.

This gives the potential for higher spikes of intensity. In particular, the current intensity values are two times as high as those in M1.

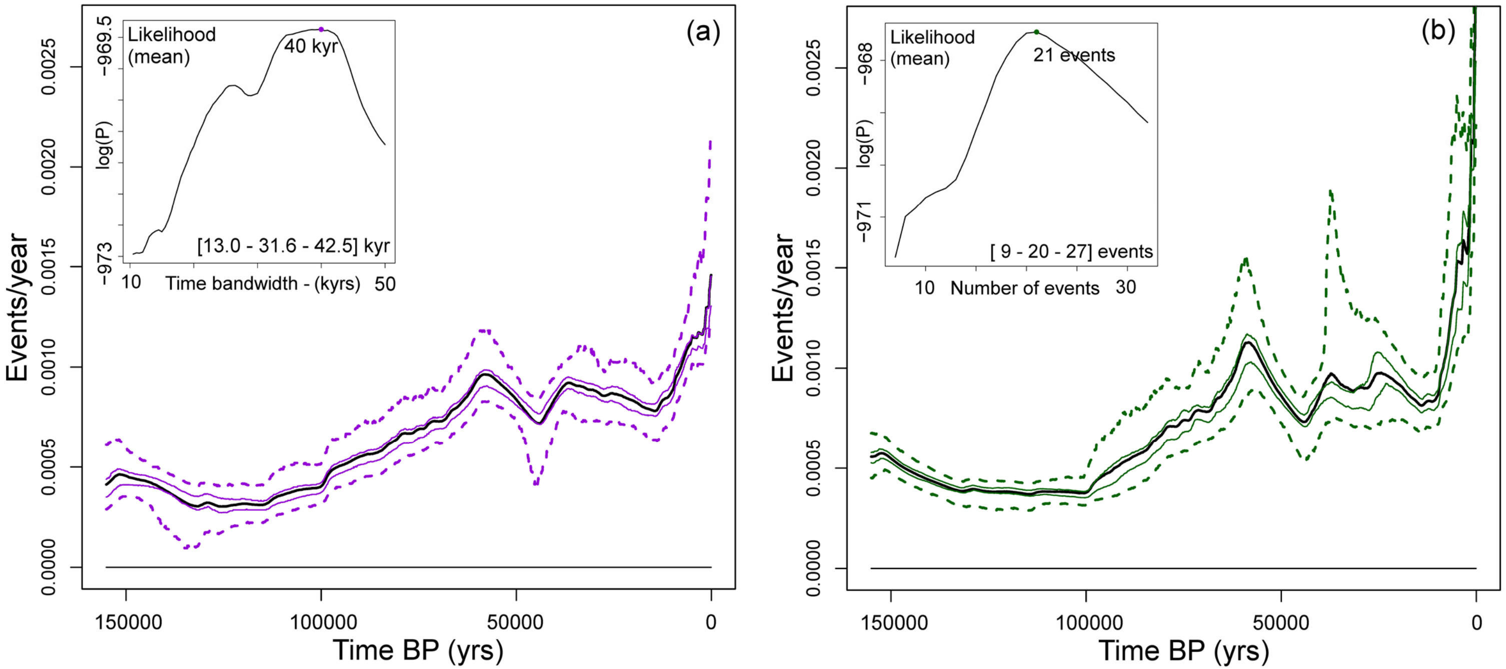

Mean curves, 5%ile, 33%ile, 67%ile, 95%ile values are displayed. Based on 1000 samples.

The bandwidth T and the number *k* are selected to maximize likelihood (MLE) of past events.

MLE can be done in the average (small boxes), or sample-wise inside a Monte Carlo simulation.

- Cox processes with self-excitement (Cox-Hawkes) -

The intensity function $\lambda(t)$ is the sum $\lambda_0 + f(t)$, where λ_0 is called base rate, and $f > 0$ is called self-excitement function.

Pre-existing events increase f with a jump Δf, and the effect of each contribution then decreases exponentially with time.

The parameter space is two dimensional:

number of clusters n, i.e. the number of ancestor events generated by the base rate λ_0

self-excitement duration τ, i.e. the time after an event before its intensity contribution Δf becomes negligible.

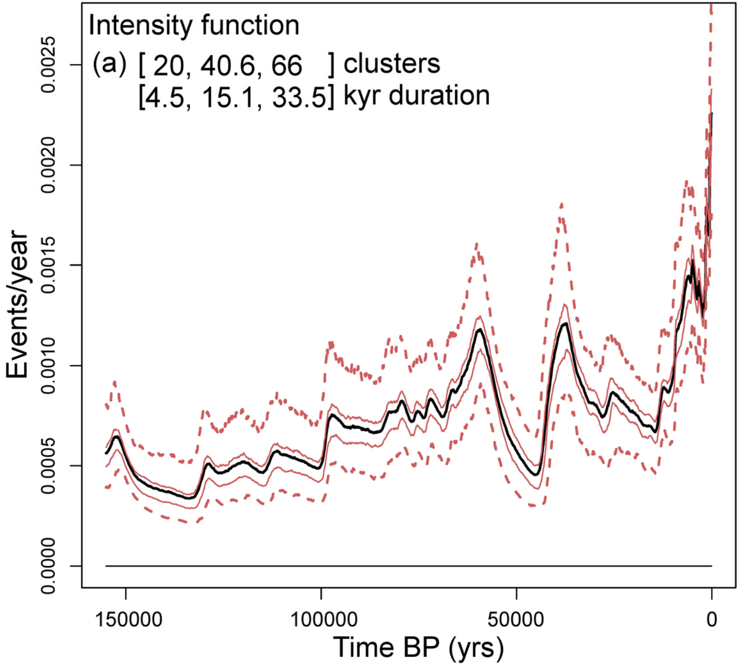

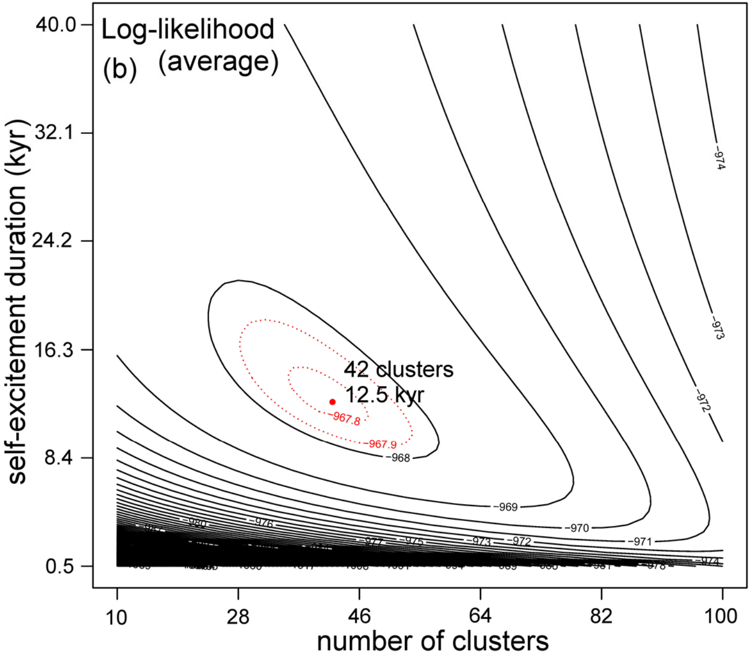

Higher spikes than in M1, but more frequent and shorter than in M1B.

A similar approach produced promising results on Campi Flegrei (Bevilacqua et al. 2016) and Auckland volcanic field (Bebbington and Cronin, 2011)

- Forecasting models results -

Our three models give different forecasts, with the current intensity $\lambda(t = 0)$ smallest in M1 and biggest in M1B.

The table shows the probability estimates of an eruption in the next 10 and 50 years, with uncertainty.
These results are preliminary.

Two alternative multi-model mixtures are displayed, based on a maximum likelihood estimator (MLE), or a Bayesian Model Averaging (BMA), with consistent results.

(a)	Model 1			Model 1B			Model 2		
	5^{th}%ile	**mean**	95^{th}%ile	5^{th}%ile	**mean**	95^{th}%ile	5^{th}%ile	**mean**	95^{th}%ile
λ [yrs^{-1}]	1/460	**1/686**	1/810	1/189	**1/344**	1/452	1/363	**1/443**	1/571
$P(\Delta t_{next}$<10 yrs)	1.23%	**1.45%**	2.15%	2.19%	**2.86%**	5.16%	1.74%	**2.23%**	2.72%
$P(\Delta t_{next}$<50 yrs)	5.99%	**7.03%**	10.31%	10.48%	**13.51%**	23.29%	8.38%	**10.67%**	12.86%
$P(MLE = M_x)$		0.4%			49.4%			50.2%	
BMA - score	0.6%	**7.5%**	22.1%	3.5%	**43.8%**	84.5%	9.6%	**48.8%**	95.7%

Based on 1000 samples.

Both methods penalize Model 1 while the others show similar performances.

(b)	MLE - selection			BMA		
	5^{th}%ile	**mean**	95^{th}%ile	5^{th}%ile	**mean**	95^{th}%ile
λ [yrs^{-1}]	1/279	**1/376**	1/473	1/289	**1/393**	1/488
$P(\Delta t_{next}$<10 yrs)	2.09%	**2.62%**	3.52%	2.03%	**2.51%**	3.39%
$P(\Delta t_{next}$<50 yrs)	10.03%	**12.45%**	16.40%	9.73%	**11.96%**	15.86%

MLE approach always follows only the model which maximizes performance, sample wise.

BMA linearly averages the models, weighting in proportion to their hind-casting performance.

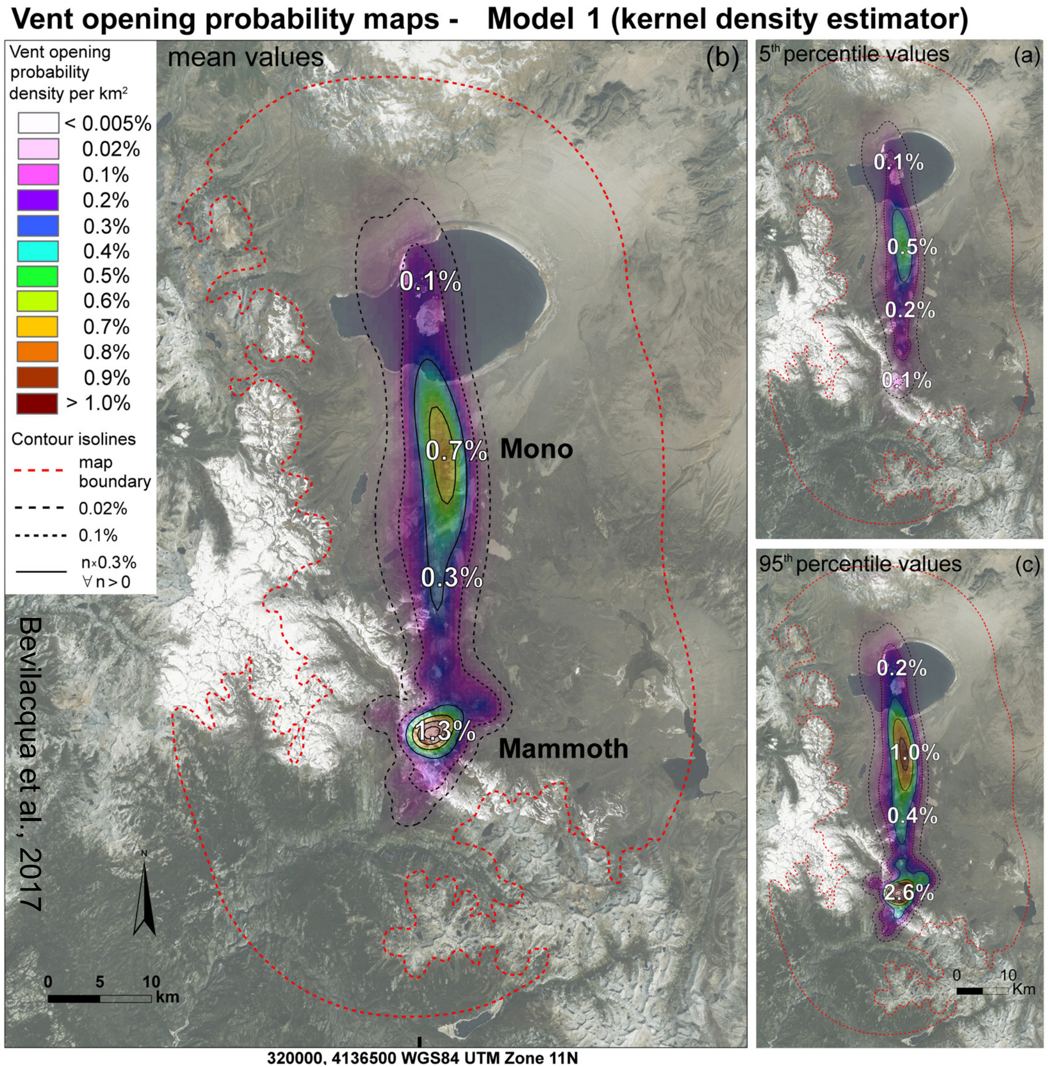

- Vent opening maps -

A "map of vent opening" is the spatial estimate of the probability of vent opening per km^2 in each point.

This probability is conditional on the occurrence of a new eruption, without a temporal window.

The forecasts are affected by uncertainty: we calculate the mean, 5th and 95th percentile values of the vent opening pdf.

MODEL 1

A new event propagates from one preexisting vent, to a random distance according to a Gaussian kernel.

Importance of vent locations belonging to the Mammoth Mountain region ranges from a negligible value to equal importance with the ones in the more recently active Mono region.

See Bevilacqua et al., 2017 for more details on the bandwidth selection method.

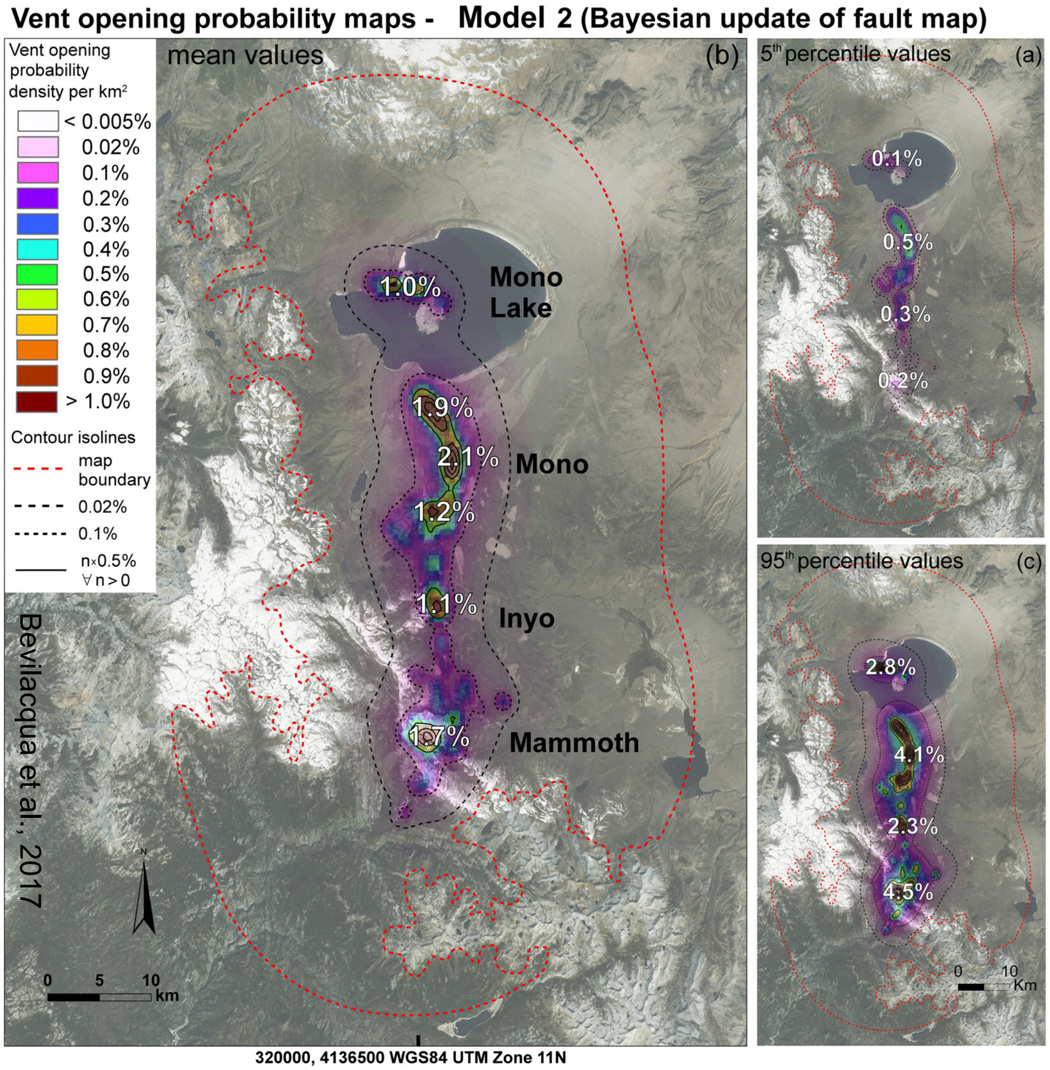

- Vent opening maps -

MODEL 2

The model assumes that the new vents will likely open near the location of a fault outcrop ζ.

The prior probability distribution of ζ comes from log-extension data younger than 130 ka.

The Bayes Theorem enables us to calculate the posterior probability density of ζ assuming Gaussian likelihood functions around past vents locations.

It describes the fault locations that are closer to past vents.

The vent opening map is then obtained by convolving the likelihood function with the distribution of ζ.

See Bevilacqua et al. 2017 for more details, including the description of the uncertainty sources.

- Vent opening maps -

Vent opening probability maps - Averaged model

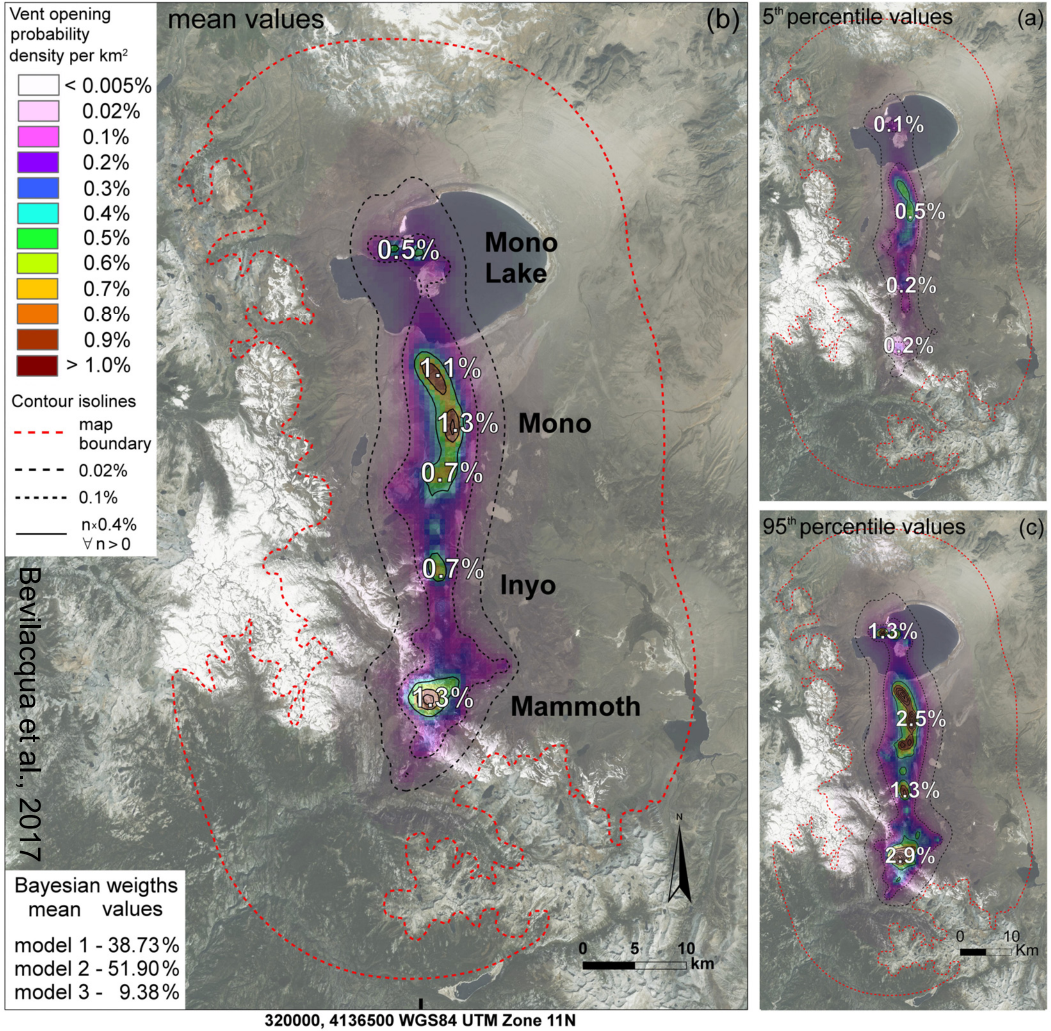

The BMA scores are proportional to the likelihood that the models give to the observed data (past vent sites).

The averaged model is the linear combination of the different model results, with the performance scores as weighting coefficients.

These probability maps combine three models:

1 - kernel density around past vent locations

2 - Bayesian update of fault map

3 - uniform probability distribution on 20 km range

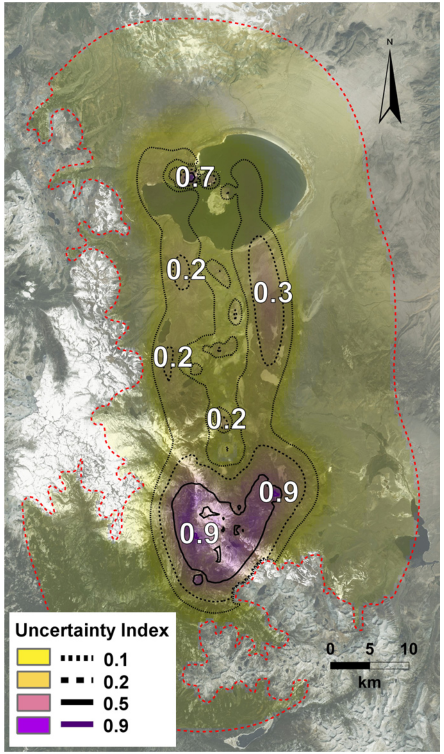

Figure (d) is the map of an uncertainty index proportional to:

(95th perc. - 5th perc.) / 5th perc.

- Summary and conclusions -

• A new probability model was developed for the effects of epistemic uncertainties affecting past eruption record.

• The procedure enabled a statistical analysis of the temporal record of Long Valley volcanic region.

• Three forecasting models were compared giving overall consistent results, with some differences.

• Two multi-model procedures were implemented to combine these forecasting models.
BMA was also applied to the vent opening mapping problem, combining three diverse models.

• This study is part of a greater project aimed at the construction of a background spatio-temporal model capable of forecasting the time and site of a future eruption in LVVR.

IAVCEI.org International Association of Volcanology and Chemistry of the Earth's Interior

IAVCEI 2017